

## Doping-induced charge redistribution in the high-temperature superconductor $\text{HgBa}_2\text{CuO}_{4+\delta}$

C. Ambrosch-Draxl, P. Süle, H. Auer, and E. Ya. Sherman  
*Institut für Theoretische Physik, Universität Graz, Universitätsplatz 5, Graz, Austria*  
 (Received 17 January 2003; published 21 March 2003)

To understand the link between doping and electronic properties in high-temperature superconductors, we report first-principles calculations on the oxygen doping effect for the single-layer cuprate  $\text{HgBa}_2\text{CuO}_{4+\delta}$ . We find ionic behavior of the dopant atom up to  $\delta=0.22$ . The excess oxygen attracts electrons from the  $\text{CuO}_2$  plane leading to an increase of the hole concentration in this building block. The maximum amount of holes is reached when the dopant oxygen shell is closed. All theoretical findings are in excellent agreement with experimental observations. We propose that this doping behavior may be a characteristic feature of high-temperature superconductors with the filling of the dopant oxygen shell to be a limiting factor for the hole content in  $\text{CuO}_2$  planes. Possible effects of the charge redistribution on  $T_c$  are discussed.

DOI: 10.1103/PhysRevB.67.100505

PACS number(s): 74.62.Dh, 74.25.Jb, 74.72.Jt

It is commonly believed that the charge carriers responsible for the superconducting pairing of high- $T_c$  cuprates are holes mainly confined to the  $\text{CuO}_2$  layers. Similar correlations between  $T_c$  and  $n_s/m^*$ , with  $n_s$  and  $m^*$  being the charge-carrier density and the effective mass, respectively, do not only include high  $T_c$  materials, but also other families of superconductors.<sup>1</sup> A universal relationship between  $T_c/T_c^{max}$  and the hole content  $p$ , exhibiting a common feature among the  $p$ -type high- $T_c$  superconductors, was presented in Ref. 2. This dependence is characterized by a plateau, where the variation of  $T_c/T_c^{max}$  is independent of the compound considered.

In all these materials the actual amount of holes is driven by doping. However, for most of the theoretical models describing the superconducting phase transition the hole content rather than the doping level is the crucial input parameter. Above all, hardly anything is known about the relationship between these two physical quantities. Without a detailed knowledge of how doping influences the number and the character of carriers in the normal state, also the superconducting properties will lack a profound understanding. In view of being able to tune the amount of carriers and thereby the superconducting transition temperature a full clarification of how doping affects the electronic structure is not only highly interesting, but even inevitable. In this context the following questions are raised: (i) Where does the excess charge go upon doping? (ii) How does doping influence the carrier concentration in the copper-oxygen planes? (iii) What limits the amount of holes in these building blocks? (iv) How does the density of states (DOS) behave as a function of doping?

In order to address these topics, we have carried out electronic structure calculations based on density-functional theory. For that purpose, we have chosen the simplest representative of the Hg-based high- $T_c$  compounds, the  $\text{CuO}_2$  single-layer  $\text{HgBa}_2\text{CuO}_{4+\delta}$  (Hg1201). This family of layered structures with the formula unit of  $\text{HgBa}_2\text{Ca}_{n-1}\text{Cu}_n\text{O}_{2n+2+\delta}$  (Ref. 3) represents the class of superconducting materials with the highest transition temperature so far. It reaches a value of 136 K for  $n=3$  which can be even enhanced by applying pressure.<sup>4</sup> Upon adding some excess oxygen,  $T_c$

can be dramatically increased.<sup>3</sup> For Hg1201, a systematic study over a wider range of doping ( $0.03 \leq \delta \leq 0.4$ )<sup>5</sup> revealed a paraboliclike  $T_c$  dependence on the oxygen content  $\delta$  exhibiting a maximum at  $\delta_{opt} \approx 0.22$ . More recent data suggested a smaller  $\delta_{opt}$  close to 0.18 (Ref. 6) or to 0.13 (Refs. 7 and 8). At optimal doping  $T_c$  is close to 97 K for ambient pressure. At 24 GPa,  $T_c$  reaches 118 K, which is the highest value of any single-layer cuprate. Although the mercury based high- $T_c$  compounds are not explicitly included in the experimental analysis described above<sup>1,2</sup> one can expect them to fit into this very general framework.

Theoretically, doping effects in this class of materials have been studied for a high doping level of  $\delta=1/2$  only<sup>9,10</sup> revealing covalent bonding in the basal Hg-O plane with large overlap of the Hg and the dopant oxygen orbitals. This oxygen concentration, however, has never been achieved experimentally. Therefore, a detailed study of the much more important lower doping regime is highly desirable. In our investigations special emphasis is put to the doping-induced redistribution of the hole concentration in the  $\text{CuO}_2$  layer. In addition, the doping effect on the crystal structure is studied.

For the investigation of the doping-dependent electronic structure, we treat the doping by using a series of supercells containing one excess oxygen atom. Oxygen concentrations of  $\delta=1/8, 1/6, 1/4, 2/9, 1/3$ , and  $1/2$  with cell sizes up to a ninefold single cell have been considered. The corresponding cells are depicted in Fig. 1. In a next step, we also investigate the effect of doping on the lattice parameters and atomic positions by total-energy and atomic-force calculations. For this purpose, the influence of the doping concentration is treated by adding the appropriate amount of valence electrons— $6 \times \delta$  (six electrons for the fully doped cell)—to the crystal in a single-cell calculation. To guarantee charge neutrality the corresponding positive charge was placed in a sphere at the doping oxygen site. As we will see below, this virtual crystal approach (VCA) is justified by the ionic behavior of the dopant oxygen. The crystalline data as a function of doping were taken from Ref. 6.

All calculations are carried out within the full-potential linearized augmented plane-wave (LAPW) method<sup>11</sup> utilizing the WIEN97 code.<sup>12</sup> Exchange and correlation effects are treated within the local-density approximation. The

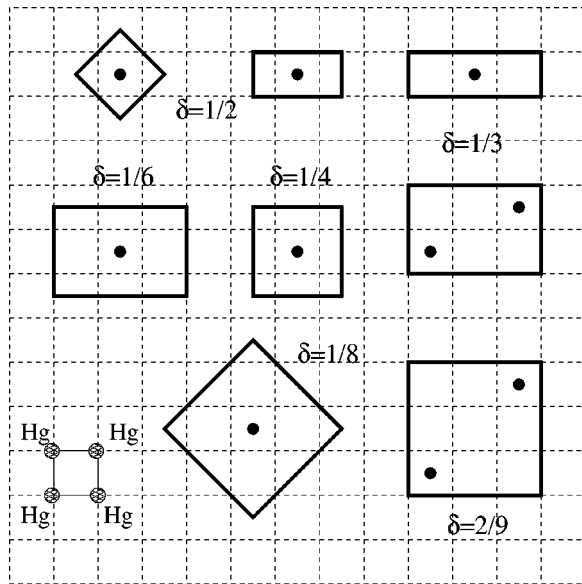


FIG. 1. Basal planes of the  $\text{HgBa}_2\text{CuO}_{4+\delta}$  supercells used for the treatment of different doping concentrations  $\delta$ . The dopant oxygen O3 indicated by the black dots is located between the Hg atoms which are exemplarily shown in the lower left corner. For  $\delta=1/3$  and  $1/2$  two different setups were used.

Brillouin-zone integrations for single-cell calculations are carried out on a  $20 \times 20 \times 8$   $\mathbf{k}$ -point mesh applying a Gaussian smearing of 0.002 mRy. Our basis set includes  $\approx 1500$  LAPW's supplemented by local orbitals for the low-lying semicore-states Hg- $5p$ , Ba- $5s$ , Ba- $5p$ , Cu- $3p$ , and O- $2s$ . For the supercell calculations the parameters were correspondingly modified. We used atomic sphere radii of 2.0, 2.2, 1.9, and 1.55 a.u. for Hg, Ba, Cu, and O, respectively. The atomiclike basis functions used within the LAPW method allow an analysis and the orbital symmetry decomposition of the electronic charge within the atomic spheres.

As already found by previous calculations carried out for the undoped material,<sup>9,13</sup> the Fermi level intersects a single free-electron-like two-dimensional half-filled  $dp\sigma^*$  band, with its states being of Cu( $d_{x^2-y^2}$ ) and O( $p_x$ ) character. Upon doping the effect on the electronic structure is twofold. First, the dopant adds states at the Fermi level, where these new charge carriers cause a shift of  $E_F$ . Second, the shift of the Fermi level changes the carrier concentration in the  $\text{CuO}_2$  plane. This can be seen in Fig. 2 where the corresponding losses in the partial charges with respect to the undoped system are displayed. The occupation number for the copper  $d_{x^2-y^2}$  orbital  $Q(d_{x^2-y^2})$  is decreased by 0.08  $e$  (from 1.442  $e$  for the undoped case to 1.362  $e$  for  $\delta=0.22$ ), and similarly the O1( $p_x$ ) charge  $Q(p_x)$  drops by 0.02  $e$  (from 0.972 to 0.952). Both orbitals clearly show a linear decrease of charges (increase of amount of holes) and exhibit their minimum occupation number (maximum number of holes) at  $\delta=0.22$ . The hole concentration within the copper-oxygen planes with respect to the undoped case obtained by  $[Q(d_{x^2-y^2})(0) + 2 \times Q(p_x)(0)] - [Q(d_{x^2-y^2})(\delta) + 2 \times Q(p_x)(\delta)]$  is also displayed in Fig. 2. Its value at  $\delta=0.22$  is 0.12  $e$ . One should note that the partial charges

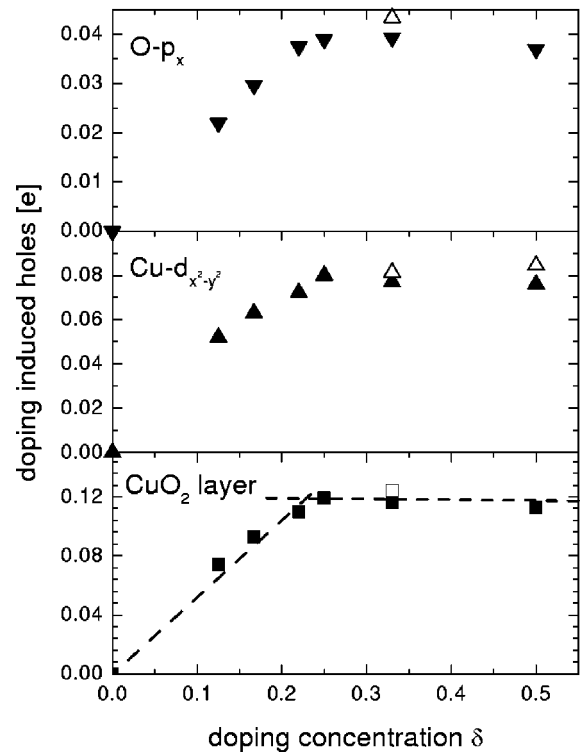


FIG. 2. Doping induced changes in the partial charges within the atomic spheres of Cu (lower panel) and O1 (middle panel), and total amount of holes (upper panel) in the  $\text{CuO}_2$  plane as a function of the doping concentration  $\delta$  obtained by supercell calculations. The open symbols indicate the alternative supercells for  $\delta=0.33$  and  $\delta=0.5$  as shown in Fig. 1. Note that in the supercells nonequivalent Cu and O positions, respectively, appear, therefore the numbers given above are averaged values.

depend on the atomic sphere radii and therefore the absolute values are somewhat bigger. The maximum hole concentration can be estimated by comparison to the charges of those states which are completely filled. By this procedure we find a value of 0.16  $e$  which is in excellent agreement with experiment.<sup>5,14</sup> In the overdoped region, we observe a plateau in parallel to the superconducting transition temperature.

The redistribution of the electron density upon doping is a complex process since the bonds exhibit covalent but also ionic character depending on the structural elements and atoms involved. Therefore the bonding of the crystal cannot be understood within a pure ionic model, especially since the  $\text{CuO}_2$  planes show strong covalent character. At the same time, however, the increase of the hole content can be understood by ionic behavior<sup>15</sup> of the dopant: The excess oxygen attracts electrons from the copper-oxygen plane thereby increasing the hole concentration in this region. The band structures of the supercells show a flat oxygen band at  $E_F$  with vanishing admixture of Hg- $d$  orbitals. These states are found at somewhat lower energy. The total and partial densities of states for  $\delta=1/4$  are shown in Fig. 3. It exhibits covalent bonding of Cu and O1 with peaks at  $-0.35$  eV and a small feature right below  $E_F$ . Covalent bonds are also formed by Hg and the apical oxygen O2, whereas the dopant atom O3 has hardly any common feature with mercury. This

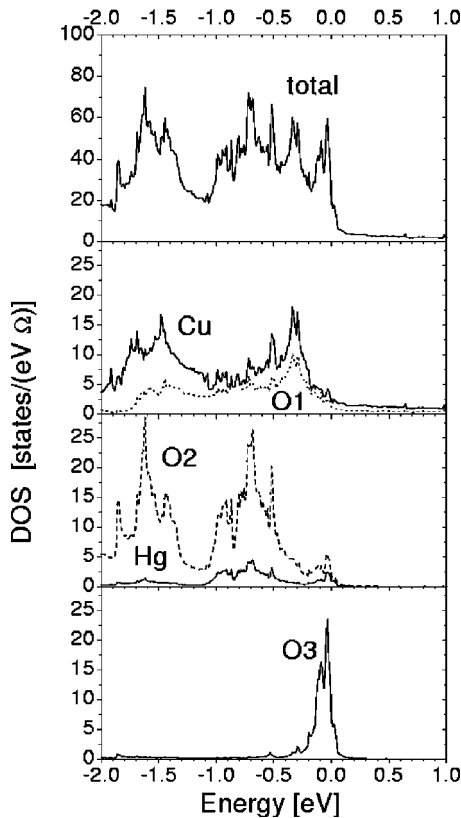


FIG. 3. Total and site-projected densities of states in states per eV and unit cell volume  $\Omega$  for  $\delta=0.25$  obtained by a supercell calculation containing one O3 atom per four formula units. (The Fermi level is set to zero.)

fact is supported by the partial charges in the Hg sphere which are not affected by doping. However, in the overdoped region, investigated for  $\delta=0.5$  and 1, rather weak covalent bonds between oxygen and mercury atoms are formed as was also found in the three-layer compound for the heavily oxygenated material.<sup>10</sup>

The ionic behavior of O3 is also supported by the fact the usage of an alternative supercell, e.g.,  $\delta=1/3$  has a very minor effect on the charge distribution (see Fig. 2). It also justifies the above described approximate description of the doping atoms within the virtual-crystal approach, which makes arbitrary doping concentrations feasible. For comparison to the supercell results, we show the doping-induced

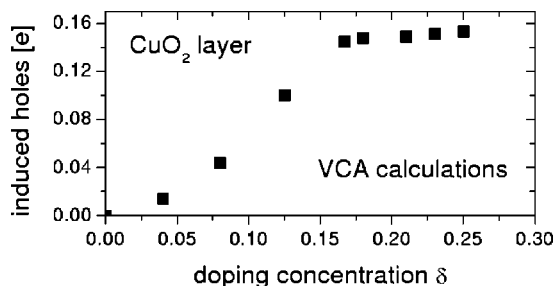


FIG. 4. Number of doping-induced holes in the  $\text{CuO}_2$  plane as a function of the doping concentration  $\delta$  obtained by VCA calculations.

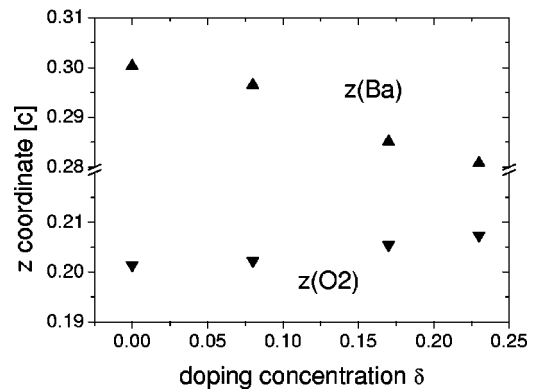


FIG. 5. Doping-induced changes in the atomic positions of Ba and O2 in units of the lattice parameter  $c$  as function of doping.

holes as obtained by this procedure (Fig. 4). Again a linear behavior as a function of  $\delta$  is found followed by a plateau. Let us turn now to the question what the limiting fact for the creation of holes in the  $\text{CuO}_2$  plane is? We propose that the hole concentration in the cuprate planes reaches its maximum when the dopant band is completely occupied, i.e., for a *closed O3 shell*. Since the excess oxygen attracts electrons from the  $\text{CuO}_2$  plane, its orbitals will be systematically filled up not only by the electrons provided by the oxygen atom itself, but also by those coming from the  $\text{CuO}_2$  unit. In order to support our hypothesis, we have repeated our VCA calculations with a muffin-tin radius of 2.5. a.u. for the O3 atom. This sphere is big enough to contain a free oxygen ion and therefore allows the interpretation of the charges inside this sphere as absolute occupation numbers. We indeed find a closed shell at  $\delta=0.22$ , corresponding to  $\delta_{opt}$  of Ref. 5.

These findings also show up in the density of states which in the optimal doping regime exhibits a filled band right below  $E_F$ . The calculated DOS at the Fermi level  $N(E_F)$  has a maximum at  $\delta=0.22$ . It contains large contributions from the  $\text{CuO}_2$  plane, but also a considerable amount of apical oxygen. All the contributions peak at  $\delta=0.22$ . From the density of states at  $E_F$  the electronic specific-heat coefficient can be determined. Assuming a similar behavior for other high- $T_c$  materials like the Bi-based compounds, the measured specific-heat coefficient  $\gamma$  of  $\text{Bi}_2\text{Sr}_2\text{CaCu}_2\text{O}_{8+\delta}$  as a function of doping<sup>16</sup> can be understood by the pronounced increase of the DOS around optimal doping. Moreover, the calculated maximum value of  $\gamma=4.4$  mJ/(mol K<sup>2</sup>) is in excellent accordance with experimental values for other high- $T_c$  materials at optimal doping.<sup>17</sup>

Not only the electronic properties, but also the crystal structure is influenced by doping. The redistribution of bond

TABLE I. Crystalline data as a function of doping obtained from total-energy and atomic-force calculations.

$\delta$	$a$ (Å)	$c$ (Å)	$\Omega$ (Å <sup>3</sup> )	$z(\text{Ba})$ [c]	$z(\text{O2})$ [c]
0.00	3.8574	9.7228	144.6676	0.3003	0.2014
0.08	3.8192	9.8191	143.2211	0.2965	0.2023
0.17	3.8058	9.6887	140.3283	0.2851	0.2055
0.23	3.8312	9.5604	140.3280	0.2808	0.2074

lengths can again be explained within the ionic picture. Since doping does not change the symmetry of the crystal, it only leads to displacements of Ba and the apical oxygen in  $z$  direction. With increasing oxygen content at the doping site, the positive Ba ions are expected to be attracted by the oxygen, whereas the negatively charged O2 ions should be repelled. Indeed a shift of the Ba position towards the basal plane is observed together with a displacement of the O2 ions away from this plane. In Fig. 5 the corresponding  $z$  coordinates of both atoms are shown which were calculated by fully optimizing the crystalline data for selected doping concentrations within the VCA: For  $\delta=0, 0.08, 0.17,$  and  $0.23$  the unit cell volumes,  $c/a$  ratios, and atomic positions were obtained by total-energy and atomic-force calculations using a similar procedure like in Ref. 18. The results are displayed in Table I. All trends are in agreement with experimental observations:<sup>6,8</sup> These are a shrinkage of the unit cell upon doping, a shortening of the lattice parameter  $a$ , an increase of  $c$  for small doping levels followed by a nearly linear decrease, an increasing distance between the basal plane and the Ba layer, as well as a reduction of the distance between the layers of Ba and O2. In agreement with measured data of Refs. 6 and 8, the latter two quantities show a less pronounced dependence at small  $\delta$  and a stronger one for higher oxygen contents.

While an agreement between structure data of different publications and our results exists, there is no consensus on the experimental  $\delta_{opt}$  value. If the hole content in the CuO<sub>2</sub> planes and  $N(E_F)$  are the main factors which determine  $T_c$ ,

our calculations support the claim of Ref. 5. However, new experimental work is needed to clarify the role of competing material-related effects like the presence of other defects.<sup>6,7</sup>

In summary, we have investigated the relationship between doping and electronic and structural properties in the high-temperature superconductor HgBa<sub>2</sub>CuO<sub>4+ $\delta$</sub> . We find that for doping concentrations up to  $\delta=0.22$  the dopant does not form covalent bonds with the neighboring Hg atoms, but shows ionic behavior, i.e., the doping oxygen adds states close to the Fermi level showing pure O3 character. Due to its high electronegativity the excess oxygen attracts electrons from the CuO<sub>2</sub> plane resulting in a redistribution of charge carriers and an increase of the number of holes in this plane. The doping-induced charge redistribution is accompanied by a shrinkage of the unit cell and displacements of Ba and the apical oxygen O2 towards and from the basal plane, respectively. The amount of holes created in the CuO<sub>2</sub> plane is limited by the closing of the oxygen shell. We conclude that this behavior may be a general feature of high- $T_c$  compounds. Further experimental investigations, however, are desirable to finally clarify the relationship between doping, hole content, and  $T_c$ .

This work was supported by the Austrian Science Fund, Projects Nos. P13430, P14004, and M591. We appreciate very stimulating discussions with J. O. Sofo. P.S. acknowledges conversation with J. Pipek and A. Zawadowski. We are grateful to M. V. Klein for bringing Refs. 7 and 8 to our attention.

<sup>1</sup>Y.J. Uemura *et al.*, Phys. Rev. Lett. **66**, 2665 (1991).

<sup>2</sup>H. Zhang and H. Sato, Phys. Rev. Lett. **70**, 1697 (1993).

<sup>3</sup>S.N. Putilin *et al.*, Nature (London) **362**, 226 (1993).

<sup>4</sup>L. Gao *et al.*, Phys. Rev. B **50**, 4260 (1994).

<sup>5</sup>Q. Xiong *et al.*, Phys. Rev. B **50**, 10 346 (1994).

<sup>6</sup>Q. Huang *et al.*, Phys. Rev. B **52**, 462 (1995).

<sup>7</sup>O. Chmaissem *et al.*, Physica C **241–243**, 805 (1998).

<sup>8</sup>A.M. Balagurov *et al.*, Phys. Rev. B **59**, 7209 (1999), and references therein.

<sup>9</sup>D.J. Singh, Physica C **212**, 228 (1993).

<sup>10</sup>D.J. Singh and W.E. Pickett, Phys. Rev. Lett. **73**, 476 (1994).

<sup>11</sup>O.K. Andersen, Phys. Rev. B **12**, 3060 (1975).

<sup>12</sup>P. Blaha, K. Schwarz, and J. Luitz, Computer Code WIEN97, (Technical University, Vienna, 1999).

<sup>13</sup>C.O. Rodriguez, N.E. Christensen, and E.L. Peltzer y Blancá, Physica C **216**, 12 (1993).

<sup>14</sup>E. Pellegrin *et al.*, Phys. Rev. B **53**, 2767 (1996).

<sup>15</sup>A.M. Abakumov *et al.*, Phys. Rev. Lett. **80**, 385 (1998).

<sup>16</sup>J.L. Tallon and J.W. Loram, Physica C **349**, 53 (2001).

<sup>17</sup>N. M. Plakida, *High-Temperature Superconductivity* (Springer, Berlin, 1995).

<sup>18</sup>R. Kouba, C. Ambrosch-Draxl, and B. Zangger, Phys. Rev. B **60**, 9321 (1999).